Conjugate observation of periodic VLF emissions near L=6

CONJUGATE OBSERVATION OF PERIODIC VLF EMISSIONS NEAR $L=6$

Hisao YAMAGISHI, Hiroshi FUKUNISHI,

National Institute of Polar Research, 9–10, Kaga 1-chome, Itabashi-ku, Tokyo 173

Toshiharu KOJIMA, Takeo YOSHINO

University of Electro-Communications, 5–1, Chofugaoka 1-chome, Chofu-shi, Tokyo 182

and

Roger GENDRIN

Centre de Recherches en Physique de l'Environnement, Terreste et Planétaire, CNET, 3 Avenue de la République, 92131 Issy-les-Moulineaux, France

Abstract: Conjugate observation of VLF emission was carried out at Kitdalen (69.1°N, 20.3°E geographic, 65.5°N, 105.3°E geomagnetic, $L=6.0$) in Norway and at Syowa Station (69.0°S, 39.6°E geographic, 66.2°S, 70.5°E geomagnetic, $L=6.1$) in Antarctica in February 1980, and also at Andøya (69.2°N, 16.0°E geographic, 66.0°N, 102.2°E geomagnetic, $L=6.1$) in Norway and at Syowa in March 1982.

During these campaign periods, periodic VLF emissions were often observed at both stations in opposite hemispheres. A typical periodic emission event observed at both stations was chosen for cross spectral analysis of the emission period. The results show the characteristics of "symmetrical three-phase emission" reported by BRICE (Radio Sci., **69D**, 257, 1965) as three wave packets, which were symmetrically spaced along the line of force, were echoing in the magnetosphere.

Though the geomagnetically conjugate point of Syowa is located about 1800 km far from Kitdalen or Andøya, the common nature of the emissions observed at both stations suggests that the periodic emission which originates from the common source in the magnetosphere can spread more than 1800 km at the ionospheric level. This observational result is compared with the ray tracing calculation. It is concluded that if the periodic emissions are guided by a field-aligned duct and the duct is terminated at an altitude of 6000 km, the periodic emissions can spread as far as the observed distance.

1. Introduction

Discrete VLF emissions excited at regular intervals are called periodic emissions. This type of emission was reported first by DINGER (1957) and the spectral structures of periodic emissions were studied by GALLET (1959), POPE and CAMPBELL (1960) and BRICE (1962). Conjugate observation of periodic emissions was reported first by LOKKEN *et al.* (1961), who showed that emissions appeared alternately at Knob Lake

(67.5°N, 1°E geomagnetic) and Byrd (68.7°S, 8°W geomagnetic) in Antarctica. HELLIWELL (1963) observed periodic emissions and whistlers successively, and he found that the repetition period of periodic emissions is the same as the two-hop group delay of whistlers. Therefore, he suggested that periodic emissions are whistler mode waves triggered near the magnetic equator by whistler mode wave packets echoing between the two hemispheres along the field lines.

BRICE (1965) found periodic emissions occurring at intervals much less than the bounce period of the whistler mode wave. This type of emission is called symmetrical multiphase emission. It is found that the emission period is usually half or one-third of the bounce period of the whistler mode wave. Therefore, he suggested that multiple wave packets spaced symmetrically along the field line are excited simultaneously in the magnetosphere. He also suggested that three-phase emissions are stable, while two-phase emissions are unstable in the magnetosphere. Actually two-phase emissions are rarely observed, and the duration is short.

In this paper we first summarize the occurrence characteristics of periodic emissions observed at Syowa Station (69.0°S, 39.6°E geographic, 66.2°S, 70.5°E geomagnetic, $L=6.1$) in Antarctica, at Kitdalen (69.1°N, 20.3°E geographic, 65.5°N, 105.3°E geomagnetic, $L=6.0$) and Andøya (69.2°N, 16.0°E geographic, 66.0°N, 102.2°E geomagnetic, $L=6.1$) in Norway during two conjugate campaigns of VLF emission observation carried out in February 1980 and March 1982.

Among these emissions, one event observed on February 26, 1980 was found to have an exceptionally short repetition period and a very good periodicity. This was a good example of three-phased periodic emissions introduced by BRICE (1965). The propagation characteristics of this emission in the magnetosphere are investigated by a cross spectral analysis of the repetition period for those stations in the opposite hemispheres.

It is interesting to note that there have been observed many events of periodic emissions in both hemispheres during the above-mentioned observation periods, although one station is separated by 1800 km from the magnetic conjugate point of the other, and so these periodic emissions are inferred to have spread widely on the ground. The size of this spreading is estimated by ray tracing calculation under the assumption that the emissions are guided by a field aligned duct and the duct is terminated at a certain altitude.

2. Presentation of the Data

During two conjugate campaigns for observation of VLF emissions in February 1980 and March 1982, many periodic emissions were observed at Kitdalen, Andøya and Syowa Station. Table 1 summarizes the occurrence of periodic emissions, in which N and S denote the ones observed in Norway and at Syowa, respectively. In February 1980, the VLF receiver at Syowa suffered severe interference from the power line system, so the weak emissions were masked by the noise. This is a reason why only a small number of periodic emissions were found during that period. The total number of periodic emission events observed in Norway or at Syowa during these periods is 21, within which those observed in the both hemispheres amount to 8.

Table 1. Summary of the occurrence of periodic emissions observed during two congugate campaign periods of February 1980 and March 1982. N and S denote the occurrence of periodic emission in Norway and Syowa, respectively.

	Date	04 UT	08	12	16
1980	Feb. 24		N		
	26		N S		
1982	Mar. 1	N	N		
	5			N S	
	6	S	S		
	8		N S	N S	
	9	N S	N		
	10		N	N S	
	11		N		
	12			N	
	14		N S		
	15			N S	
	16			S	
	17		S		
	19		N		
	23	N			

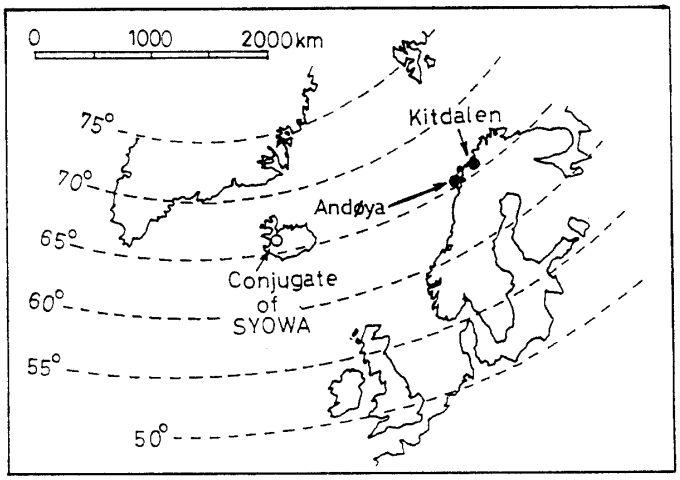

Fig. 1. Relation between Kitdalen and Andøya in northern Norway (solid circle) and the geomagnetic conjugate point of Syowa Station, Antarctica (open circle). Dashed lines show geomagnetic latitude. These points are in the same geomagnetic latidude but they are separated by 1600–1800 km longitudinally.

Therefore, the probability of simultaneous occurrence of periodic emission in northern Norway and Syowa is 38% of the total periodic emissions. Figure 1 shows the locations of Kitdalen, Andøya and the magnetic conjugate point of Syowa. The distance from the conjugate point of Syowa to Kitdalen and to Andøya is 1800 km and 1600 km, respectively. Periodic emissions are considered to propagate along field-aligned ducts. So, the probability of 38% seems to be very high considering the long distance between the conjugate point at Syowa and the observation points.

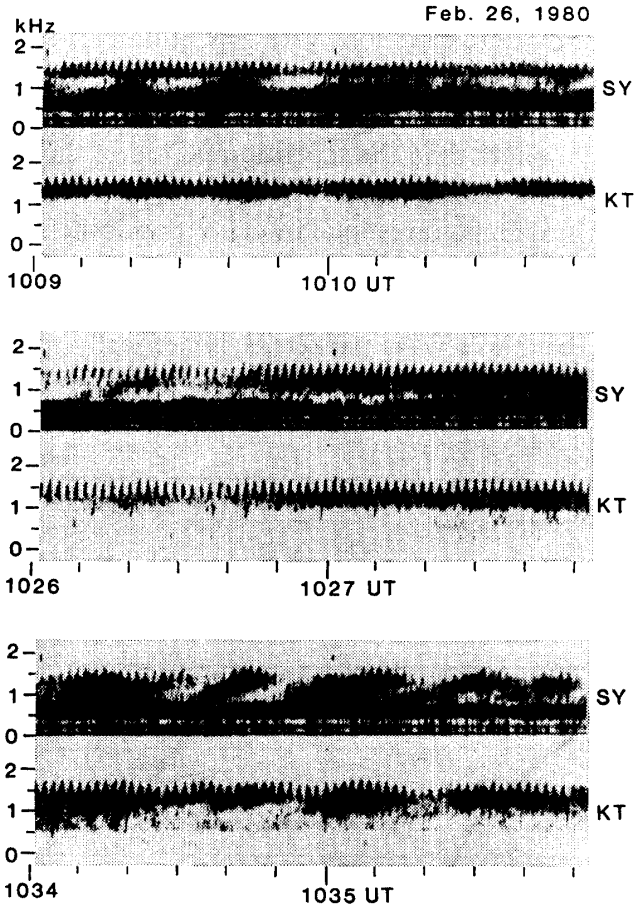

Fig. 2. Frequency-time display of VLF emission observed on February 26, 1980 at Syowa (SY) and at Kitdalen (KT). Rising-tone emissions with repetition period of 20 s are quasi-periodic emissions and a series of discrete emissions with repetition period of 1.7 s are periodic emissions.

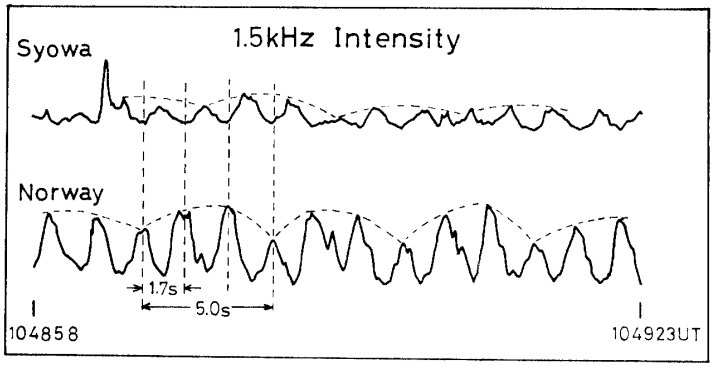

Fig. 3. An example of periodic emission, which shows regular intensity variation such as every third emission is weaker than others.

In this paper, we analyze the one observed on February 26, 1980 among these periodic emissions. This event was observed at Kitdalen and at Syowa as shown in the frequency-time spectra in Fig. 2, and it shows the most prominent periodicity.

In Fig. 2, rising-tone emissions with repetition period of 20 s are quasi-periodic emissions and a series of discrete emissions with repetition period of 1.7 s are periodic emissions.

Further, it is found that the intensity of discrete emissions is sometimes modulated with a period three times longer than the repetition period of the emissions. Figure 3 shows the time variation of 1.5 kHz intensity from 1048: 58 to 1049: 23 UT. It is clearly seen that every third emission is much weaker than others so that the envelope of the emission intensity illustrated by dashed lines has a period of 5 s. The vertical dashed lines in Fig. 3 show that the emissions appeared alternately at both stations. These features suggest that three wave packets, symmetrically spaced along the propagation path, are echoing in the magnetosphere, as reported by BRICE (1965).

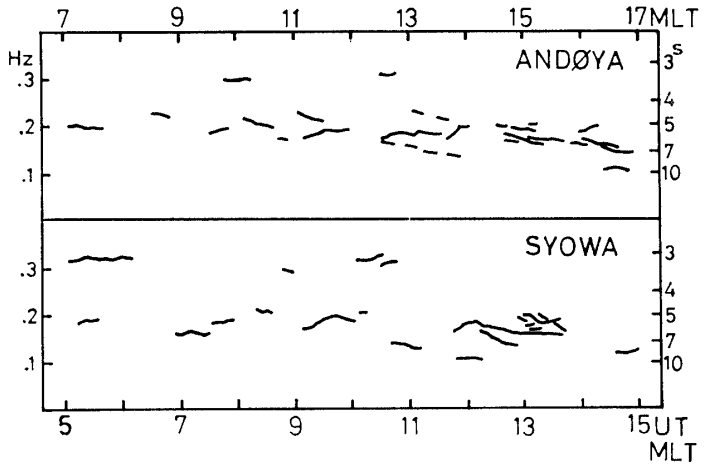

Fig. 4. Summary of the repetition period of periodic emissions observed in March 1982 as a function of magnetic local time.

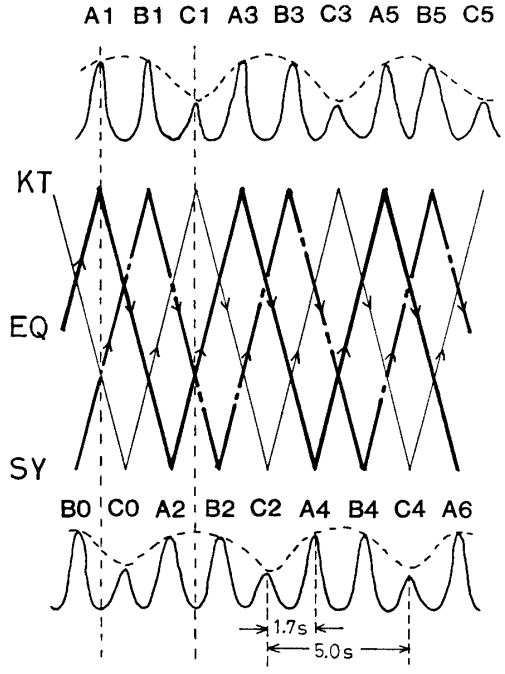

Fig. 5. Schematic illustration of the motion of three wave packets echoing between opposite hemispheres, and expected wave forms of their intensity variation on the ground.

In that case, the real bounce period of wave packets becomes 5 s (three times fo 1.7 s). Actually the 1.7 s period is very short compared with other periodic emissions observed in these campaigns. Figure 4 summarizes the repetition period of periodic emissions observed in March 1982 as a function of magnetic local time. It ranges from 3 to 10 s with the medium around 5 s. Therefore, it is very likely that the periodic emission observed on February 26, 1980 formed a symmetrical three-phase emission. The motion of the three wave packets and the emission intensity expected on the ground are schematically illustrated in Fig. 5. Here the symbols A, B, C denote three different groups, and suffix 0 to 6 denote the sequence of reflection at each hemisphere.

3. Cross Spectral Analysis for the Repetition Periods

Cross spectral analysis is carried out for 1.5 kHz intensity of the periodic emission observed on February 26 in the time interval of 1048: 58 to 1049: 23 UT given in Fig. 3. Maximum Entropy Method (MEM) of the 15th order is applied to the data of 3 Hz sampling with analysis time lag of 5 s. The results are shown in Fig. 6. The top panel shows the power spectra for Syowa and Kitdalen, and the bottom panel shows the phase and the coherency spectrum between these two stations.

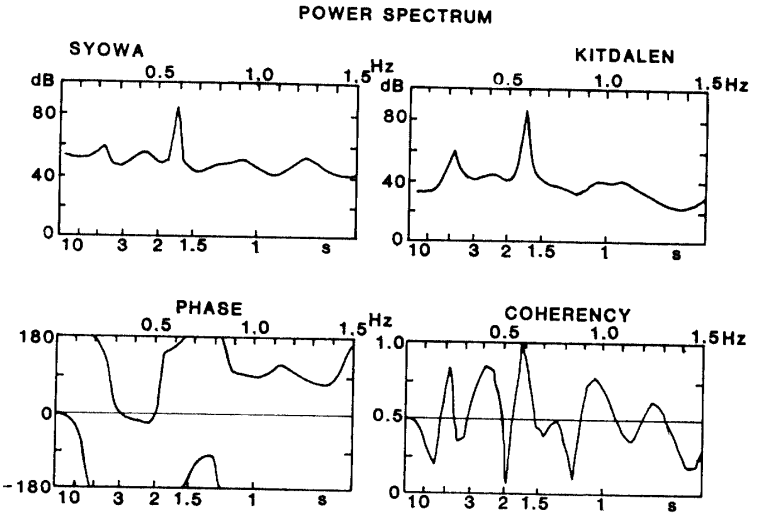

Fig. 6. A result of cross-spectral analysis for 1.5 kHz emission intensity at Syowa and Kitdalen. Power spectra at Syowa and Kitdalen are shown in the top panel. Three wave packets form apparent bounce period of 1.7 s. Fundamental period of 5 s is also recognized. The phase and the coherence spectrum are shown in the bottom panel. For 1.7 and 5 s periods, the phase relation is out of phase, which is easily expected from the diagram in Fig. 5. In the coherence spectrum, the harmonic structure of the repetition period is greatly enhanced.

The spectral peaks in the periods of 5 s (0.2 Hz) and 1.7 s (0.6 Hz) are clearly seen in the power spectra of both stations. The former corresponds to the bounce period of whistler mode waves along the $L=6$ line of force, and the latter seems to be an apparent bounce period formed by three sets of wave packets. The phase relation of these periods is almost out of phase in the Syowa-Kitdalen pair, which is consistent with the motion of wave packets illustrated in Fig. 5.

Besides these spectral peaks, a small one at 2.5 s is recognized in the power spectra. The coherency spectrum in the bottom panel shows that coherency is high at 2.5 s as well as 5 and 1.7 s. However, it is difficult to find out a relation between the 2.5 s period and the motion of wave packets in the magnetosphere. Therefore, it is likely that this is the second harmonic of the distorted wave form of 5 s period illustrated by a dashed-curve in Fig. 3. Note that the spectral peak at 1.7 s (the third harmonic) is greater than that at 5 s (fundamental). It is also interesting that there is no second harmonic component of the 1.7 s period component, though this component was much stronger than the 5 s component. It may be due to the fact that the wave form of the 1.7 s component was much more sinusoidal, compared with the 5 s component, as seen in Fig. 5. These characteristics are different from usual harmonic structure,

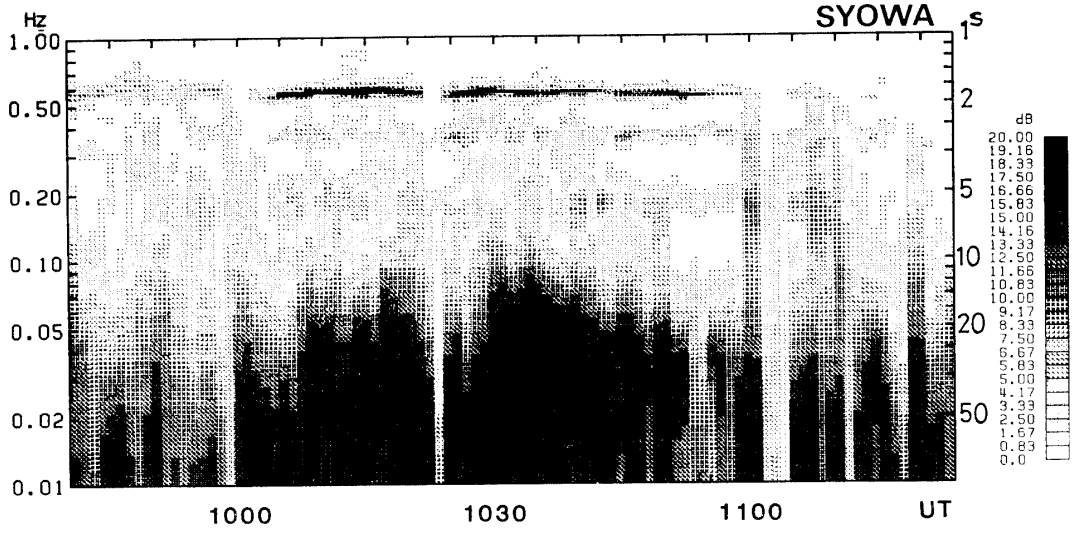

Fig. 7. Time variation of power spectra of emission intensity of 1.5 kHz at Syowa. Narrow-band component at 1.7 s period corresponds to periodic emission and broad-band component in the period range 15–50 s corresponds to quasi-periodic emission.

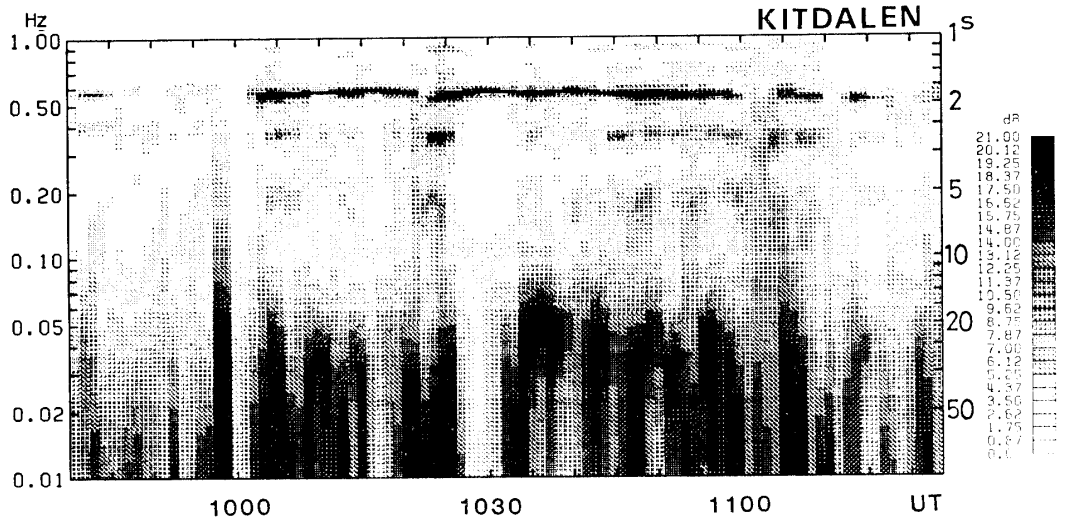

Fig. 8. Same as Fig. 7 except for the observation station to be Kitdalen.

and are useful to distinguish multiphase periodic emissions from usual ones.

In order to study the time variation of the emission period and the phase relation between the two hemispheres, the dynamic spectra were calculated in the time interval of 0920–1150 UT by the 30th order MEM with analysis time lag of 15 s and the data window of 2 min. The results are given in Figs. 7–11. Figures 7 and 8 show time variation of the repetition period observed at Syowa and Kitdalen, respectively. Broad-band spectral components in a period range of 15–50 s correspond to quasi-periodic (QP) emissions, while a narrow-band spectral component with a period of 1.7 s corresponds to the periodic emissions. Figure 9 is the same as Fig. 8 except for the expanded frequency scale. It is found that the repetition period increases gradually with magnetic local time from 1.7 s at 1000 UT (1225 MLT) to 1.9 s at 1125 UT (1350

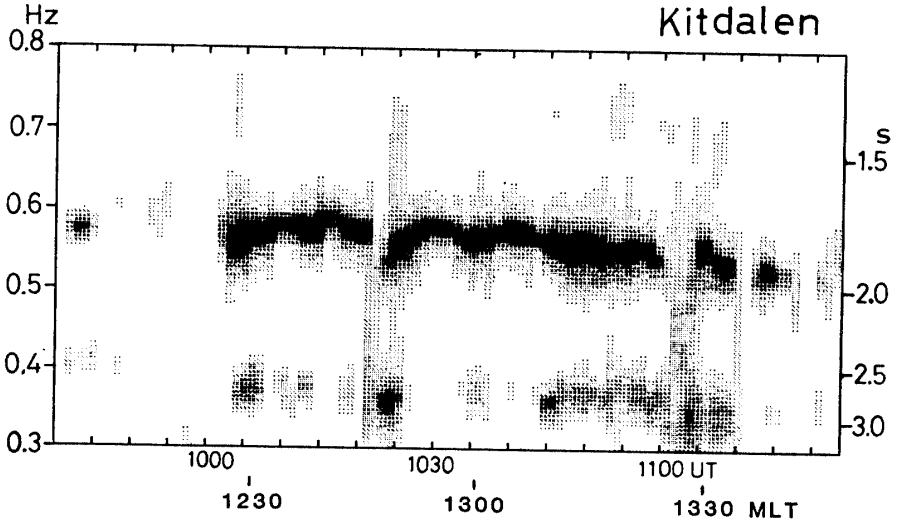

Fig. 9. Same as Fig. 8 except for expanded frequency scale. Gradual increase of the repetition period with magnetic local time, from 1.7 s at 1225 MLT to 1.9 s at 1350 MLT, is recognized.

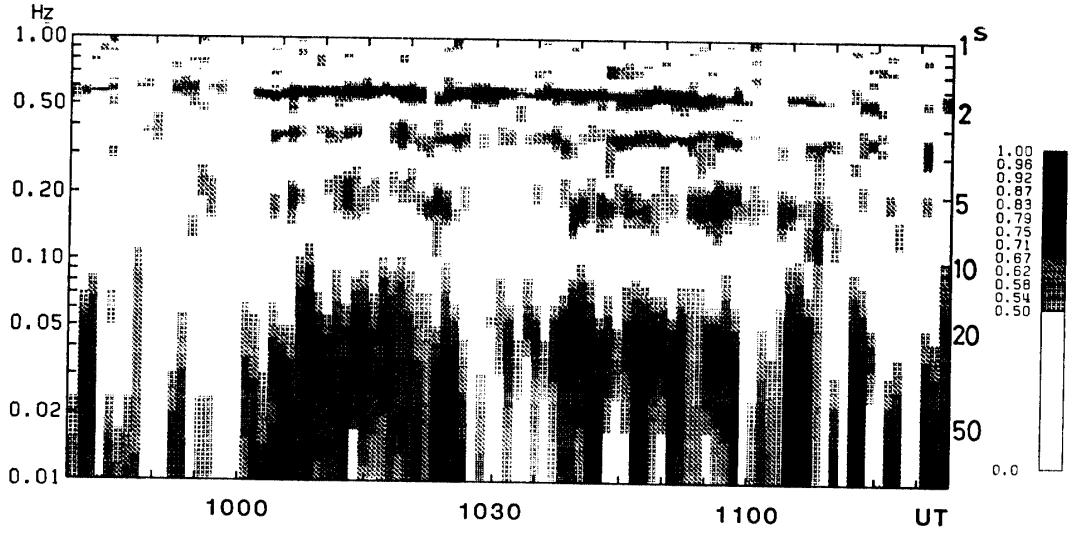

Fig. 10. Time variation of coherency of 1.5 kHz emission intensity between Syowa and Kitdalen.

MLT).

This tendency is also recognized in Fig. 4. The group velocity of whistler mode wave is inversely proportional to the square root of the electron density along the propagation path. So, if the electron density increases with local time in the dayside magnetosphere as often observed by GEOS satellites (*e.g.* DÉCRÉAU *et al.*, 1982), the group velocity of whistler mode wave is decreased and the bounce period of the wave is increased with local time.

In Figs. 7 and 8 the fundamental period of 5 s is hardly seen. This fact indicates that in general the intensities of three wave packets included in the bounce period of 5 s are not much different although the example of three wave packets with significant intensity difference is presented in Fig. 3. The periodicity at 5 s, however, is evident in the frequency-coherency spectrum given in Fig. 10, in which the coherency of the 1.5 kHz intensity variations between Syowa and Kitdalen is displayed in gray scale. The harmonic structure at 5, 2.5 and 1.7 s is greatly emphasized in Fig. 10. Therefore, it is suggested that the frequency-coherency spectrum is quite useful for finding out multiphase periodic emission events.

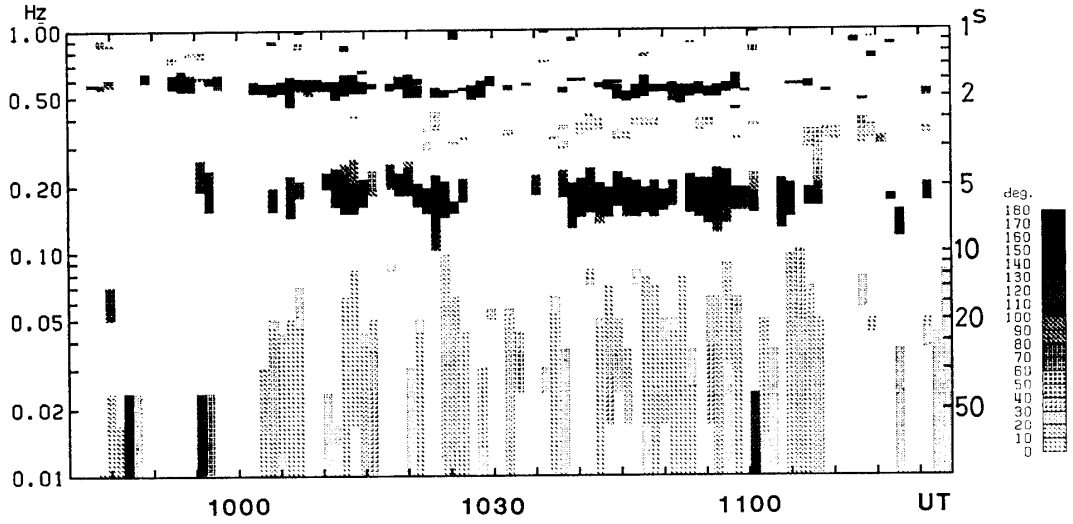

Fig. 11. Time variation of the phase relation of 1.5 kHz emission between Syowa and Kitdalen. A dark color represents the out-of-phase (180°) relation.

Figure 11 gives the phase relation of the 1.5 kHz intensity variations between Syowa and Kitdalen in gray scale. A dark color represents the out-of-phase (180°) relation. Only the spectral components with coherency higher than 0.5 are displayed in the figure. It is found that the fundamental and the third harmonics have always the out-of-phase relation, and the second harmonic has the in-phase relation.

4. Discussions

The existance of symmetrical three-phase periodic emission, first reported by BRICE (1965), is reconfirmed in this paper. During the VLF observation in February 1980 and March 1982, we could find more than 20 periodic emission events, but only

one three-phase emission was found among them. Besides, the periodicity of this three-phase emission is very good compared with other periodic emissions. Therefore, some unusual condition seems to be required to cause multiphase emissions. The generation mechanism of multiphase emissions is an interesting problem, but further discussion is difficult within the limitation of these ground VLF emission data alone. So, we proceed to discuss another important fact that the conjugacy of periodic emission is very good for those station pairs separated a long distance from their magnetically conjugate points.

The regular repetition periods of periodic VLF emissions suggest that these waves are propagating along a field-aligned wave guide and bouncing in the magnetosphere. In that case, periodic emissions are most likely to be observed at magnetically conjugate points in opposite hemispheres. In our observation, however, periodic emissions were often observed at those station pairs separated 1600–1800 km from their conjugate points. Such a tendency is also found in the paper of BRICE (1965) which reported

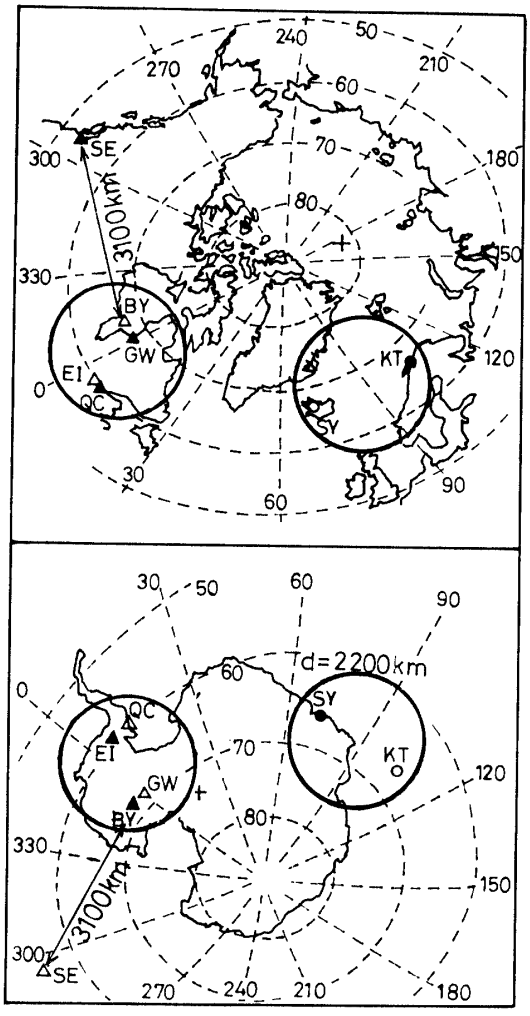

Fig. 12. Spatial relation of VLF stations where periodic emissions were simultaneously observed. The stations are marked by solid circles and triangles and their geomagnetic conjugate points are also shown by open ones.

that periodic emissions with frequencies of 1.2–1.7 kHz were observed simultaneously at two conjugate pairs of stations, Quebec City and Eights, Great Whale River and Byrd. These two conjugate pairs are separated by 1000 km in latitude and 500 km in longitude. In another case, periodic emissions with frequencies of 2.5–3 kHz were observed at Seattle and Byrd. The conjugate point of Byrd is located 3100 km far from Seattle.

The locations of these stations are summarized in Fig. 12. The conjugate points of the stations are represented by open circles and open triangles. Geomagnetic coordinates are also shown by dashed lines in the figure. If the wave frequency is higher than the cutoff frequency of the wave guide mode confined between the ionosphere and the ground, the wave can propagate over a long distance with small attenuation. This cutoff frequency is about 2 kHz in the daytime. Therefore, the periodic emissions observed at Seattle and Byrd might have propagated through the ionosphere-ground wave guide. However, in other cases the emission frequencies are lower than the cutoff frequency of the wave guide mode. Thus the size of the emission region on the ground must be attributed to the spread of ray path in the topside ionosphere.

A possible explanation for this spread is that a field-aligned duct is terminated above the topside ionosphere and the waves released from this duct spread in a wide region as they propagate downward to the ground. In this model the size of spreading depends on the altitude of the duct termination. Therefore, in the following, the relation between this altitude and the size of the spreading on the ground is analyzed by

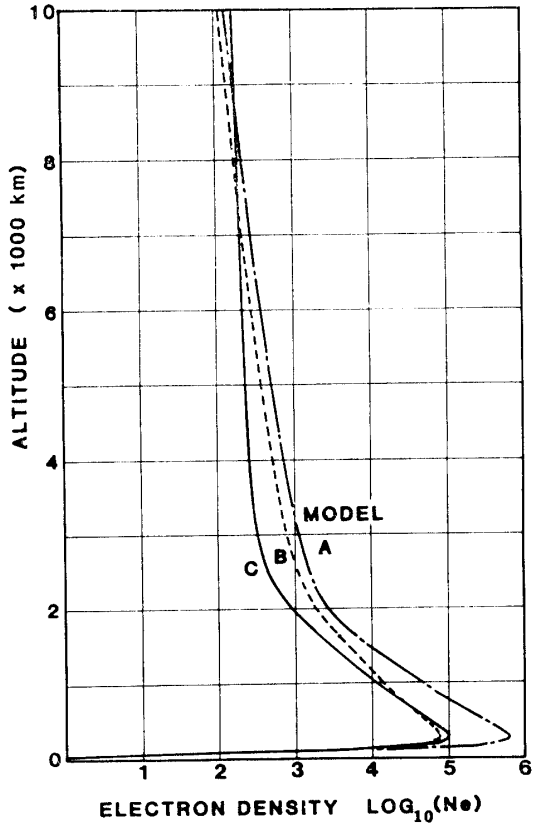

Fig. 13. Three models of electron density profile used in ray tracing.

means of ray tracing. As the stations and their conjugate points are separated not only latitudinally but also longitudinally, 3-dimensional ray tracing is required to obtain 2-dimensional spreading on the ground. However, in the case of large dip angle of geomagnetic field, the propagation in the off-meridian plane is not much different from the one in the meridian plane. In our case the dip angle at Kitdalen or Andøya is large enough (78°), so we first obtain the latitudinal spread of ray path by 2-dimensional (meridional) ray tracing, then apply this result to the longitudinal direction.

Figure 13 shows three models of electron density profile used in the ray tracing. In models A and B, diffusive equilibrium distribution in the lower altitude and collision free distribution (BAUER, 1969) in the higher altitude are smoothly connected by arctangent function (AIKYO and ONDOH, 1971) at the altitudes of 2000 and 1430 km, respectively. The former simulates the profile in the summertime and the latter simulates the one in the wintertime. Model C is a simple diffusive equilibrium model with the reference height of 600 km and the electron temperature of 2400 K.

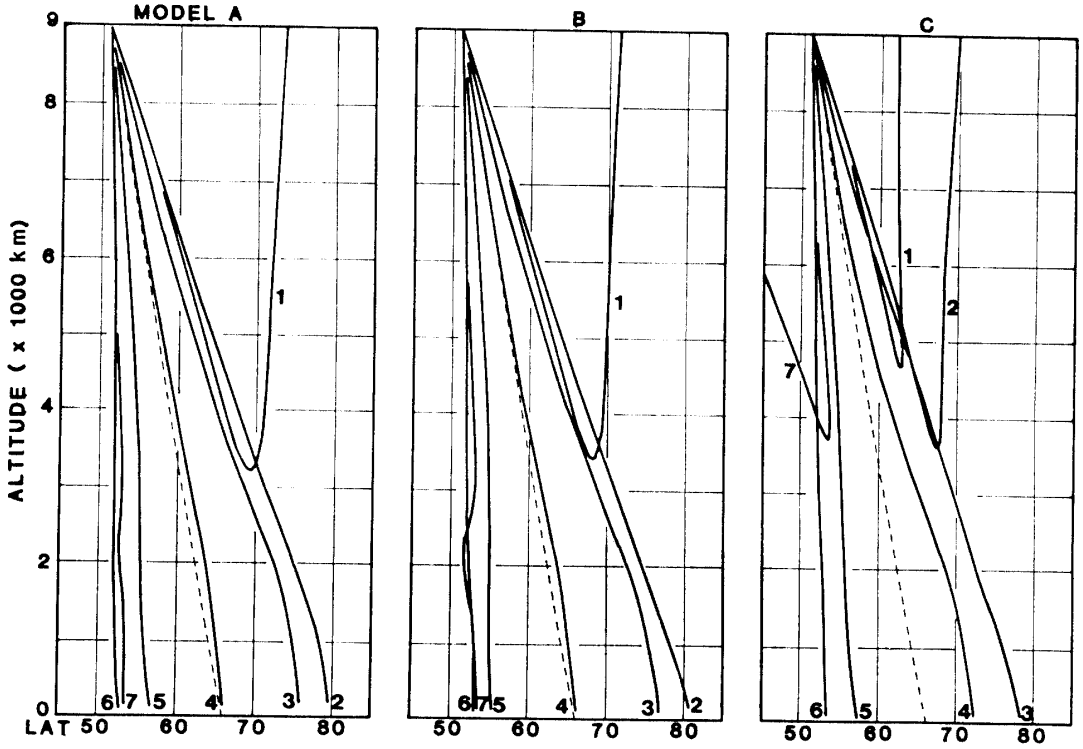

Fig. 14. Calculated ray paths from the duct termination to the ionosphere. Altitude of the duct termination, D_h, is assumed to be 9000 km at $L=6.1$. The ray paths, numbered 1 to 7, have the initial wave normal angles of 60°, 40°, 20°, 0°, −20°, −40° and −60°. The dashed line shows the $L=6.1$ line of force.

In order to obtain a relation between the altitude of a duct termination and the spread of the ray paths on the ground, we assume three altitudes, 9000, 6000 and 3000 km, in the ray tracing. In the first case, the duct termination is assumed at the altitude of 9000 km along the $L=6.1$ line of force. Figure 14 shows the ray paths of 1.5 kHz wave calculated for three electron density profiles shown in Fig. 13. The duct is

assumed to be terminated at the altitude of 9000 km, and seven initial wave normal angles are selected as $\psi_i=60°, 40°, 20°, 0°, -20°, -40°, -60°$, which correspond to the ray paths denoted by the numbers 1 to 7 in the figure. The angle ψ_i is measured from the local magnetic field, and the positive value corresponds to the wave normal directed toward the outer L shell. The range of wave normal angles to be trapped in the field-aligned electron density enhancement is dependent upon the degree of enhancement from the background density. To be able to trap the waves with $\psi_i=60°$, the required electron density enhancement is 200%, which is a rather unrealistic value. However, as there is no information on the electron density enhancement, we calculate the ray path over such a wide range of wave normal angles for completeness. Later, it will be shown that those ray paths with large ψ_i are not effective to increase the size of the spreading of the wave on the ground.

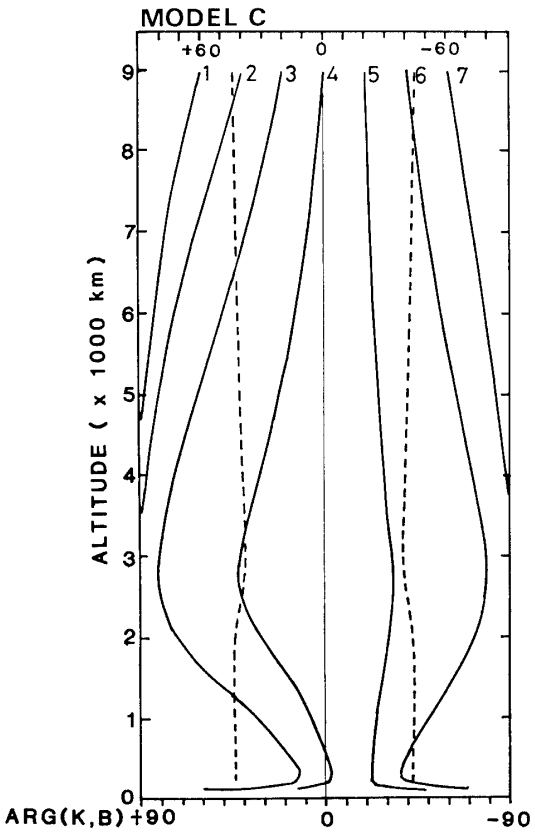

Fig. 15. Wave normal angles along the ray paths of model C in Fig. 14. The dashed line shows the inflection angle.

In Fig. 14, a ray path with $\psi_i=60°$ (numbered 1) is reflected at the altitude of 3200–3500 km in models A and B, and ray paths with $\psi_i=60°$, 40° and −60° (numbered 1, 2 and 7) are reflected in model C. This reflection is explained by the change of wave normal angles in the course of propagation. Figure 15 shows the wave normal angles along the ray paths of model C. In this figure, the wave normals for all the ray paths tend to direct away from the magnetic field as the wave propagates downwards to the 3000 km altitude, and in the case of large $|\psi_i|$ ($\psi_i=60°$, 40° and −60°),

the wave normal becomes perpendicular to the local magnetic field before it reaches the ionosphere. As the frequency of the wave (1.5 kHz) is lower than the LHR frequency in this altitude range (about 3 kHz for this model), the wave is reflected upward (KIMURA, 1966).

Model dependence of the ray paths is found in the figure, that the ray path with $\phi_i=0°$ (numbered 4) follows the $L=6.1$ line of force in models A and B, but it deviates 6° toward higher latitude in model C. The ray paths with $\phi_i=40°$ and $-60°$ (numbered 2 and 7) reach the 100 km altitude in models A and B, but they are reflected in model C. However, the range of latitude occupied by these rays at the 100 km altitude is not much different among these models (28° in models A and B, and 25.5° in model C).

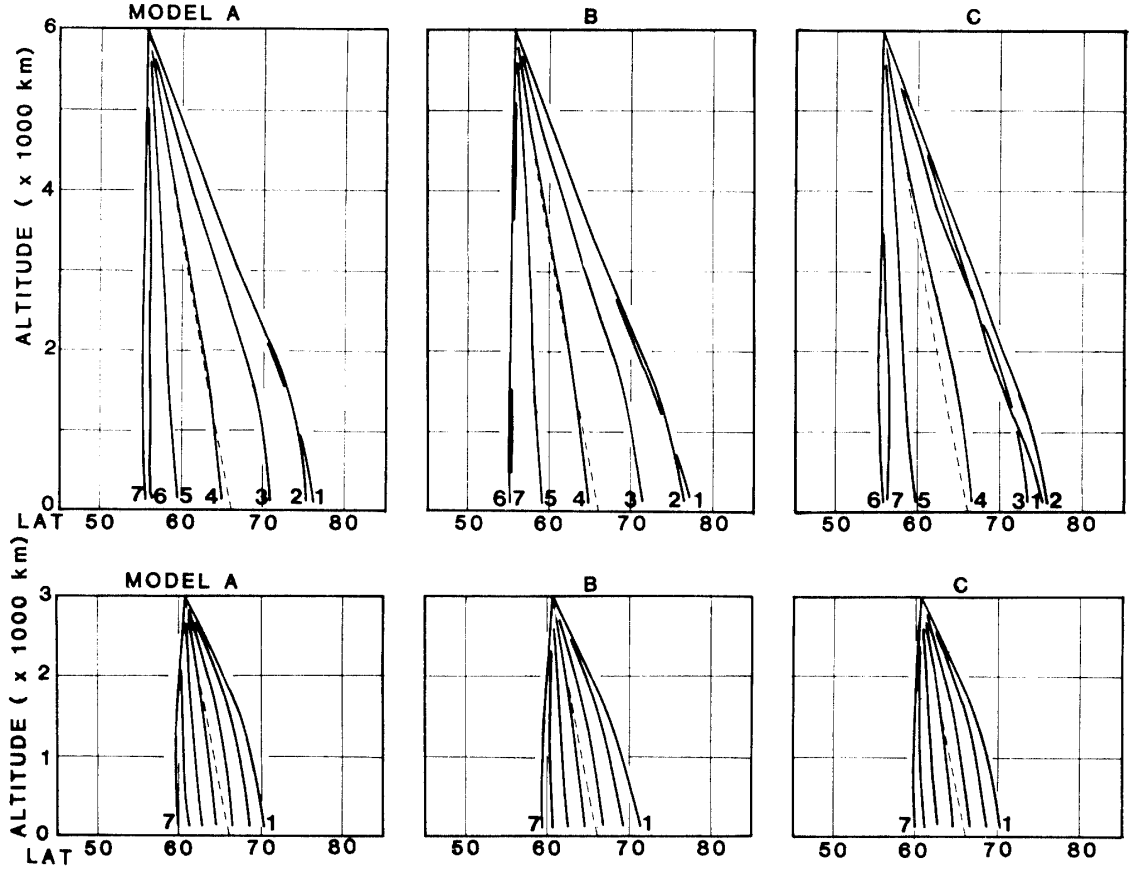

Fig. 16. Calculated ray paths from the duct termination to the ground. Altitude of the duct termination is assumed to be 6000 km (top panel) and 3000 km (bottom panel).

In the second case, the altitude of the duct termination is assumed to be 6000 km along the $L=6.1$ line of force. The ray paths with $\phi_i=60°\sim-60°$ are numbered 1 to 7 in the top panel of Fig. 16. In this figure, the arriving latitude of rays at the 100 km altitude shows a positive correlation with ϕ_i while ϕ_i is small (ray paths 3, 4 and 5), but the change of the arriving latitude becomes smaller for larger ϕ_i. When ϕ_i is large enough ($|\phi_i|\geq 40°$), the ray paths become overlapped (ray paths 1 and 2 in models A and B) or even the inversion occurs on the relation between ϕ_i and the arriving latitude

(ray paths 6 and 7 in models B and C, 1 and 2 in model C). This overlap or inversion of ray paths is also found in Fig. 14 (ray paths 6 and 7 in models A and B).

These characteristics can be understood by examining the relation between the wave normal angles and the inflection angle defined as a wave normal angle at which the deviation of the ray direction from the magnetic field shows maximum. Figure

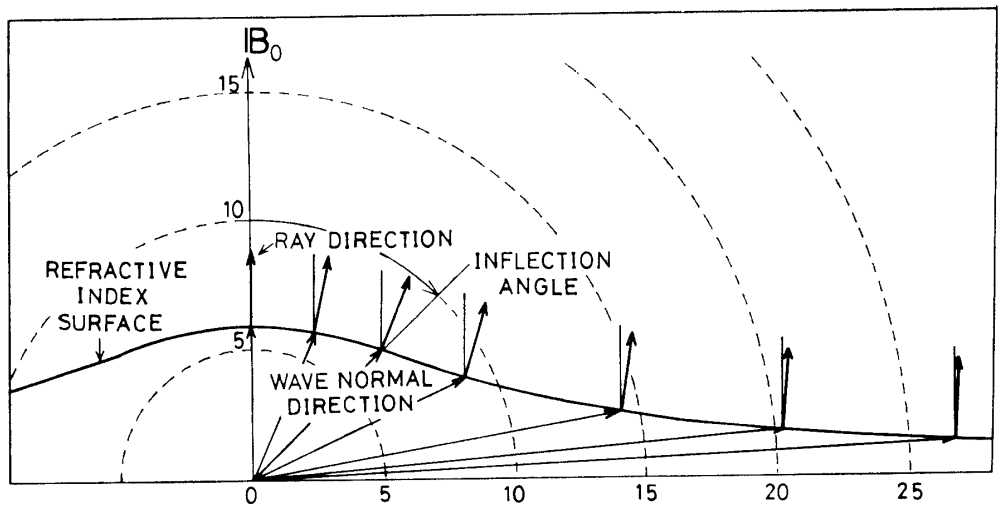

Fig. 17. The relation between the wave normal direction and the ray direction for the refractive index surface at an altitude of 3000 km.

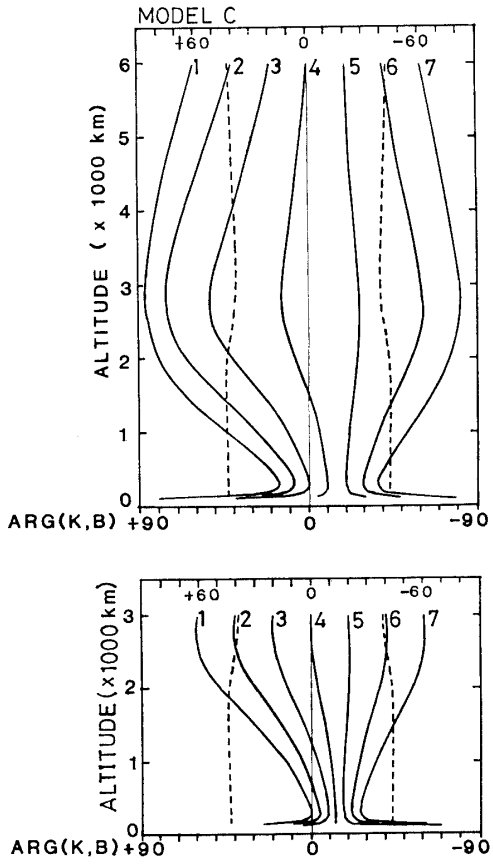

Fig. 18. Wave normal angles along the ray paths shown in Fig. 16. The altitude of the duct termination is assumed to be 6000 km (top panel) and 3000 km (bottom panel).

17 illustrates the relation between the wave normal angle and the ray direction by using a refractive index surface at an altitude of 3000 km. If the wave normal angle is smaller than the inflection angle, the ray angle increases with wave normal angle, and the ray path with larger wave normal angle shows a larger deviation from the initial magnetic line of force. However, if the wave normal angle exceeds the inflection angle, the ray angle decreases with increasing wave normal angle, and the ray path with larger wave normal angle ceases to deviate from the magnetic field line.

In the top panel of Fig. 18, wave normal angles are shown for the ray paths of model C in the top panel of Fig. 16. The inflection angles are shown by dashed curves in the figure. For the ray paths 3, 4 and 5, the wave normal angle remains smaller than the inflection angle for the most part of the propagation, so these ray paths deviate from the magnetic line of force as ψ_i increases. For the ray paths 1, 2, 6 and 7, the wave normal angle is larger than the inflection angle for the most part of the propagation, and so the ray paths with larger ψ_i tend to come closer to the magnetic field line. For this reason, the ray with large ψ_i (in this case $|\psi_i| \geq 40°$) is not effective to increase the size of the spreading of the wave on the ground, and this size is not much model dependent (the range of latitudes occupied by these ray paths is 21°, 22° and 20.4° for models A, B and C, respectively).

In the last case, the altitude of the duct termination is assumed to be 3000 km, and the ray paths and the wave normal angles with $\psi_i = 60° \sim -60°$ are shown in the bottom panels of Figs. 16 and 18. Because of the steep electron density gradient below the 2000 km altitude as shown in Fig. 13, wave normal angles approach a vertical direction to the ionosphere, or 12.5° (90°−dip angle of the $L=6.1$ field line) from the magnetic field. This effect is seen in other cases (Fig. 15 and the top panel of Fig. 18), but it is most prominent in this case, and this keeps the wave normal angles within the inflection angle for the most part of the propagation. Accordingly, there arises no overlap of ray paths for different ψ_i, nor inversion on the relation between ψ_i and the arriving latitude.

These calculations shown in Figs. 14 to 18 give a rough estimation on the spreading of ray paths in the ionosphere as a function of the altitude of duct termination. These waves usually have a larger incident angle than the acceptance cone angle at the bottom of the ionosphere, and they are totally reflected. However, the wave length of 1.5 kHz wave in free space is 200 km, which is much longer than the distance from the bottom of the ionosphere to the ground. Thus it is possible that the magnetic and electric fields of the wave leak out through the ionosphere to the ground in evanescent mode with attenuation rate of several dB (KIMURA *et al.*, 1978). Therefore, it is concluded that the size of the emission region observed on the ground is comparable to the estimated extent of ray paths at the altitude of 100 km.

The ray tracing calculation was repeated with small increment of ψ_i for three different altitudes of the duct termination, $D_h = 3000$, 6000 and 9000 km, to see the extent of ray path more precisely. Figure 19 shows the result of this calculation. The abscissa is the latitude of ray path arriving at the 100 km altitude, and the ordinate is the initial wave normal angle ψ_i at the exit of a duct. The horizontal distance measured from the foot point of the magnetic line of force at $L=6.1$ is also marked in the abscissa. Termination of the curve indicates that the ray undergoes LHR

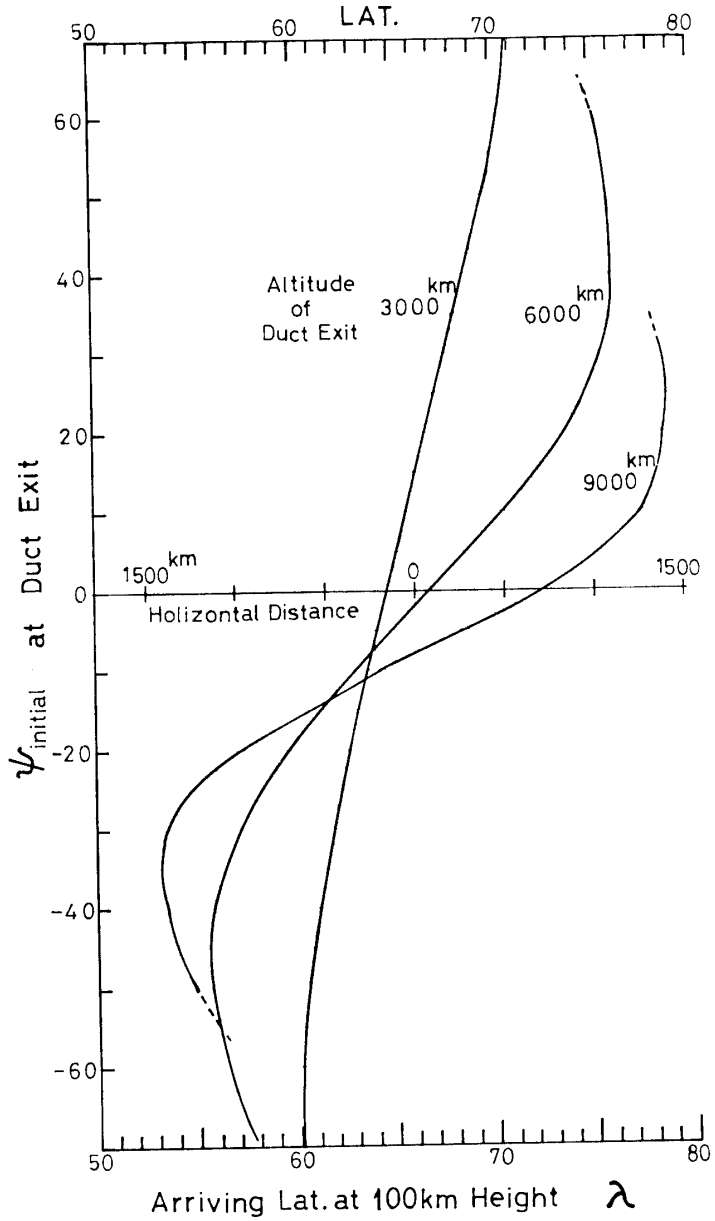

Fig. 19. Relation between the initial wave normal angle ϕ_i at the duct termination and the arriving geomagnetic latitude of ray path at the altitude of 100 km for three different altitudes of duct termination.

reflection for further increase of ϕ_i. It should be noted that there is a latitude range in which the ray path can spread at the 100 km altitude. The critical values of ϕ_i at which the ray paths show largest latitudinal deviation are 25° and −32° for D_h=9000 km, and 37° and −45° for D_h=6000 km. If D_h is higher than 6000 km, the electron density enhancement which can trap the waves in the range $-45° < \phi_i < 37°$ is about 40% from the background level. Therefore, even if the density enhancement is greater than 40%, it is not effective to increase the size of spreading at the 100 km altitude.

From these calculations the spreading of ray paths at the altitude of 100 km is estimated to be 1190, 2280 and 2880 km for D_h=3000, 6000 and 9000 km, respectively.

The spreading on the ground is almost equal to that at the altitude of 100 km as discussed before. Therefore, the size of area given in Fig. 12, in which periodic emissions originated from the common source are observed, is comparable with the spreading of ray paths when the altitude of the duct termination is 6000 km.

5. Summary

From the conjugate compaign of VLF emission observation at Kitdalen or Andøya in northern Norway and at Syowa Station in Antarctica, carried out in February 1980 and March 1982, we obtained the following results:

(1) During these campaign periods, periodic emissions are simultaneously observed in northern Norway and Antarctica with the probability of 38% out of the total 21 periodic emission events. This probability is high if we consider the fact that the stations in northern Norway are separated by 1600–1800 km from the geomagnetic conjugate point of Syowa, and it is suggested that periodic emissions are spreading more than 1800 km on the ground.

(2) The repetition period of these periodic emissions ranges 3 to 10 s with the medium around 5 s and an exception of 1.7 s observed on February 26, 1980. These periods increase with magnetic local time. This is attributed to an increase in the total electron content in the dayside magnetosphere toward afternoon hours.

(3) The periodic emission of 1.7 s repetition period observed at Kitdalen and Syowa on February 26, 1980 is studied with cross spectral analysis of the repetition period between the two stations. From the exceptional shortness and the harmonic structure of the repetition period, it is suggested that the emission consisting of three wave packets is echoing along the geomagnetic line of force. This reconfirms the existence of multiphase periodic emission reported by BRICE (1965).

(4) The inferred spreading of periodic emission described in item 1 must be attributed to the propagation effect in the magnetosphere or in the topside ionosphere since the frequency of the emission is lower than the cutoff frequency of the earth-ionosphere wave guide. From the ray path tracing in the topside ionosphere it is concluded that when the field-aligned wave guide with electron density enhancement of 40% terminates at the 6000 km altitude, the propagation paths spread over 1800 km at an altitude of 100 km and also on the ground.

Acknowledgments

We wish to express our thanks to the members of the 21st and 23rd wintering party of the Japanese Antarctic Research Expedition for their effort in the ground-based VLF observation. We also extend our thanks to the members of the GEOS-2-ground conjugate campaign carried out in February 1980 at Kitdalen, Norway for their kind cooperation. We greatly appreciate the kind cooperation of Dr. J. HOLTET in the VLF ground observation during the Japan-Norway balloon campaign of March 1982. The data processing in this work was performed by the computer system at the Information Processing Center of the National Institute of Polar Research.

References

AIKYO, K. and ONDOH, T. (1971): Propagation of nonducted VLF waves in the vicinity of the plasmapause. J. Radio Res. Lab., **18**, 153–182.

BAUER, S. J. (1969): Diffusive equilibrium in the topside ionosphere. Proc. IEEE, **57**, 1114–1118.

BRICE, N. M. (1962): Discussion of paper by R. L. DOWDEN, 'Doppler-shifted cyclotron radiation from electrons: A theory of very low frequency emission from the exosphere'. J. Geophys. Res. **67**, 4897–4899.

BRICE, N. M. (1965): Multiphase periodic very-low-frequency emission. Radio Sci. J. Res. NBS/USNC-URSI, **69D**, 257–265.

DÉCRÉAU, P. M. E., BÉGHIN, C. and PARROT, M. (1982): Global characteristics of the cold plasma in the equatorial plasmapause region as deduced from the GEOS 1 mutual impedance probe. J. Geophys. Res., **87** (A2), 695–712.

DINGER, H. E. (1957): Periodicity in dawn chorus. paper presented at IRE-URSI Symposium, 1957.

GALLET, R. M. (1959): The very low frequency emissions generated in the earth's exosphere. Proc. IRE, **47**, 211–231.

HELLIWELL, R. A. (1963): Whistler-triggered periodic VLF emissions. J. Geophys. Res., **68**, 5387–5395.

KIMURA, I. (1966): Effect of ions on whistler-mode ray tracing. Radio Sci., **1**, 260–283.

KIMURA, I., YAMAGISHI, H., MATSUO, T. and KAMADA, T. (1978): S-310JA-1 rocket observation of VLF emission spectra at Syowa Station in Antarctica. Mem. Natl Inst. Polar Res., Spec. Issue, **9**, 51–68.

LOKKEN, J. E., SHAND, J. A., WRIGHT, Sir C. S., MARTIN, L. H., BRICE, N. M. and HELLIWELL, R. A. (1961): Stanford-Pacific Naval Laboratory conjugate point experiment. Nature, **192**, 319–321.

POPE, J. H. and CAMPBELL, W. H. (1960): Observations of a unique VLF emission. J. Geophys. Res., **65**, 2543–2544.

(Received November 12, 1983; Revised manuscript received January 13, 1984)